Dynamics and Polarization Effects in small-area vertical-cavity surface-emitting Lasers in free-running Mode and with time-delayed Feedback

Markus Sondermann, Hans Bohnet, Michael Weinkath, Thorsten Ackemann

Institut für Angewandte Physik, Westfälische Wilhelms–Universität Münster,
Corrensstr. 2/4, D–48149 Münster, Germany

ABSTRACT

The polarization dynamics of vertical-cavity surface-emitting lasers operating close to threshold is investigated experimentally. For free-running devices a characterization of the dynamics is given for a scenario when two modes are excited at threshold due to a small net gain anisotropy. The polarization dynamics in this regime are found to be governed by the relaxation oscillations and to exhibit an anticorrelation of the two modes. The level of anticorrelation is strongly depending on the injection current. If isotropic feedback by a distant reflector is added, the dynamics are governed by the external cavity round-trip time scale and low frequency fluctuations are observed for both modes. These are shown to occur also for large net gain anisotropy, but without excitation of polarization degrees of freedom.

Keywords: vertical-cavity surface-emitting lasers, polarization dynamics, feedback, low frequency fluctuations

1. INTRODUCTION

Vertical-cavity surface-emitting lasers (VCSELs) are often used devices in todays information technology, especially in fiber-based communication systems as local area networks. In contrast to their edge-emitting counterparts, VCSELs exhibit some advantages that are consequences of their different cavity geometry. Due to the short cavity length, VCSELs operate in a single longitudinal mode only.[1] In addition, the fact that emission takes place in the vertical direction, i.e. in the direction of crystal growth, overcomes the geometrical constraints of edge-emitting lasers and results in a circular geometry of the active zone. This opens the possibility of circular beam profiles and thus easy coupling of the VCSEL emission to optical fibers without a huge amount of additional beam shaping optics.

However, the circular geometry does not provide a polarization preference and hence polarization degrees of freedom are easily excited. A prominent manifestation of the resulting polarization instabilities is the phenomenon of polarization switching,[2–9] i.e. a sudden change to the linear state of polarization oriented orthogonally to the one selected at threshold, if the current surpasses a critical value. On the one hand side, these polarization instabilities can set limits to device performance in potential applications.[10] But the possibility of devices that take advantage of the polarization degrees of freedom in VCSELs has been discussed also.[11]

In spite of this tendency to display polarization instabilities, most authors report the selection of a well defined state of polarization at lasing threshold.[5] This has been attributed to residual anisotropies that break the circular symmetry of the VCSEL cavity.[3] Due to birefringence, the resonance frequency of electromagnetic

---

email: sondema@uni-muenster.de, t.ackemann@uni-muenster.de

waves with orthogonal polarization is no longer degenerate. Instead, orthogonal linear polarizations are emitted in different longitudinal modes of same order but with slightly different optical frequencies. These modes will, in general, also have a slightly different net gain (net gain = unsaturated gain - unsaturated losses), which results in the selection of the favored mode at threshold.[3] In this paper, the term ‘dichroism’ will be used to denote the resulting net gain anisotropy that results from various effects like mechanical stress,[3, 7, 12] anisotropic losses in the Bragg mirrors of the VCSELs[13] and gain differences for the polarization modes due to the different material gain that is caused by the different positions of the modes on the gain curve.[3]

However, even at threshold the selection of the polarization state is not perfect in every device and under every operating condition. In a few experiments[7, 14, 15] the excitation of both orthogonal polarization modes at threshold, followed by the continuous depletion of one mode for increasing current, has been observed. In[14] this scenario has been shown to disappear for an anisotropic transverse cavity geometry in which the losses for one mode are increased. Data published in[16] show also an increase of output power in both modes at threshold. Both modes display also a similar linewidth characteristics. This behavior has been interpreted as a typical threshold behavior of the nonlasing mode and has been termed ‘anomalous spontaneous emission’. However, in none of these papers this scenario was investigated in deeper detail.

In this paper, it will be shown that for a small modulus of the dichroism both orthogonally polarized modes are lasing at threshold. We will term this regime *two-frequency emission state.* If the dichroism is changed by changing the operating conditions, i.e. by changing the substrate temperature, a continuous transition to a polarization switching scenario at higher currents is observed. The dynamics of the two modes will be shown to be anticorrelated. The strength of the anticorrelation depends on current and the characteristic time scale is the one of the relaxation oscillations.

An interesting question is, how the dynamics in this regime are affected by isotropic optical feedback, as it naturally occurs in applications like, e.g., fiber coupling. Polarized feedback was shown before to have a rather strong impact on VCSELs.[17–19] There are also several experimental publications dealing with the spectral and noise properties[20–23] of VCSELs with feedback, but – in contrast to edge-emitting semiconductor lasers – the temporal dynamics of VCSELs exposed to isotropic feedback have been only scarcely investigated.[22] In the latter paper, a scenario similar to the low frequency fluctuations (LFF) known from edge-emitting semiconductor lasers (for an overview we refer to[24]) has been demonstrated for the total output power. Theoretical considerations can be found in.[25]

In this paper we will show the existence of LFF in both of the orthogonally polarized modes, if isotropic feedback is applied to the laser in the parameter regime, in which the solitary laser shows two-frequency emission. The dominating timescale of the polarization dynamics with feedback will be shown to be governed by the external cavity round-trip time. The LFF are shown to exist also for higher values of the dichroism. As for the solitary laser, a continuous transition will be demonstrated from LFF in both modes to LFF in only one of the two polarization modes at high values of the net gain anisotropy.

The outline of this paper is as follows: In the next section the experimental setup is introduced. In Sec. 3 the experimental results for the investigations in the solitary laser are reported. The results of the feedback experiments will be given in Sec. 4. The paper will be finished with some summarizing conclusions in the last section.

2. EXPERIMENTAL SETUP

In Fig. 1 the experimental setup is displayed. The VCSELs used in the experiments are commercial gain-guided devices (Emcore Corp., Model 8085-2010). We have chosen devices with an 8 μm wide aperture in order to ensure operation in the fundamental transverse mode up to more than twice the threshold current. The VCSELs are mounted in a temperature controlled copper holder that is attached to a thermoelectric cooling system. With this home built system the substrate temperature of the VCSELs can be changed and stabilized in a range from 6°C to 70°C.

First, the setup common to the experiments with the free running laser and with feedback is explained. The light emitted from the VCSEL is collimated using an aspheric antireflection coated lens. After passing through a half wave plate ($\lambda/2$), the orthogonally polarized components of the VCSEL output are split by a Wollaston

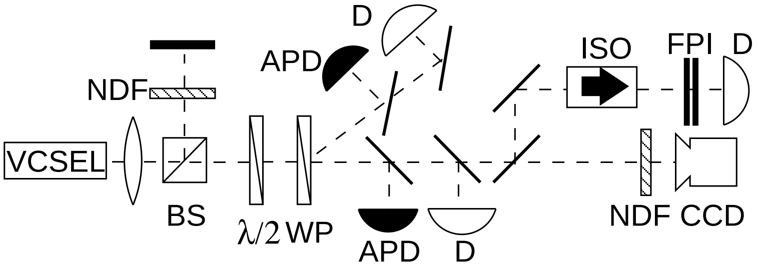

Figure 1. Experimental setup, for explanations see text.

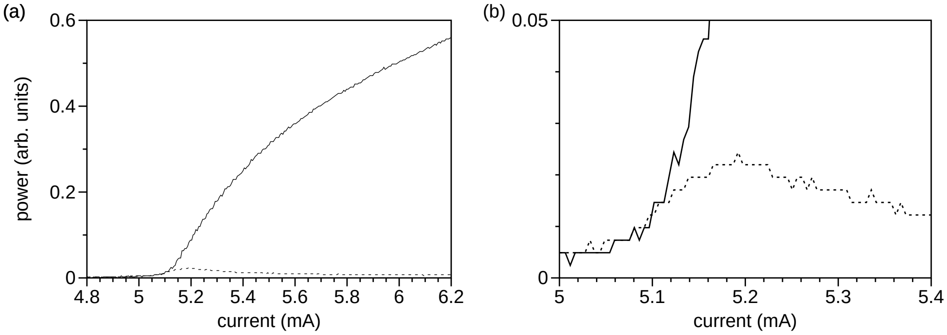

Figure 2. Polarization resolved power in dependence on the injection current (a). The power of the mode with lower (higher) optical frequency is denoted by solid (dashed) lines. In (b) a magnification of the current interval around the lasing threshold is displayed.

prism (WP). For each polarization component the time averaged output power and the temporal dynamics can be measured by a low bandwidth detector (D) and an avalanche photo diode (APD) of 1.8 GHz bandwidth, respectively. The output of the APD is recorded with a digital oscilloscope with 1 GHz analog bandwidth. Radio-frequency (RF-) spectra are measured with a PIN-diode of 10 GHz bandwidth and a power spectrum analyzer of 20 GHz bandwidth. A scanning Fabry-Perot interferometer (FPI) with a finesse better than 150 and a free spectral range of 46 GHz is used to record optical spectra. Unintended back reflections into the laser are prevented by an optical diode (ISO). Images of the near field intensity distribution are obtained by means of a CCD-camera.

For the experiments with isotropic feedback a non polarizing beam splitter (BS) is inserted between the collimation lens and the half-wave plate. The BS directs 66% of the output power onto a highly reflective mirror that closes the external cavity. The external cavity round-trip time is 3 ns. The ratio of the light reflected back into the VCSEL is controlled by means of neutral density filters (NDF). The external mirror and the position of the collimation lens are adjusted to obtain mode-matched feedback. The criterion used is the maximal threshold reduction. By measuring the Stokes parameters in each output branch of the BS we confirmed that the polarization properties of the light in the external cavity is not altered by the BS. For this measurement a zero-order quarter-wave plate was used in addition to measure the circularly polarized fraction of the light.

3. DYNAMICS AT THRESHOLD IN THE SOLITARY LASER

Figure 2 shows the polarization resolved power as a function of the injection current of one of the devices under study. At lasing threshold, both of the orthogonally polarized modes start to lase with equal time averaged power. The optical spectrum at the lasing threshold (Fig. 3) exhibits two peaks with orthogonal linear polarization, i.e. the observation of power in both polarization directions cannot be attributed to emission of a single elliptically polarized mode. The amplitude and width of the two peaks are of comparable magnitude. Hence, we term this state ‘two-frequency emission state’.

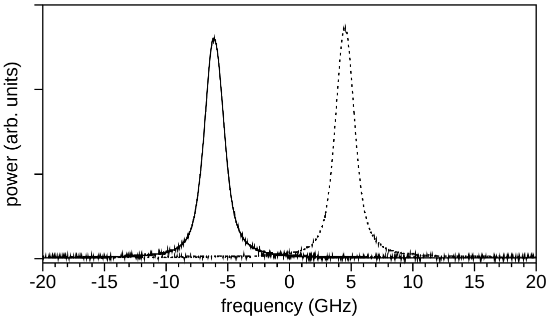

Figure 3. Polarization resolved optical spectrum at the lasing threshold (5.08 mA). The spectrum for projection onto the polarization direction corresponding to the mode with lower (higher) optical frequency is denoted by solid (dashed) lines.

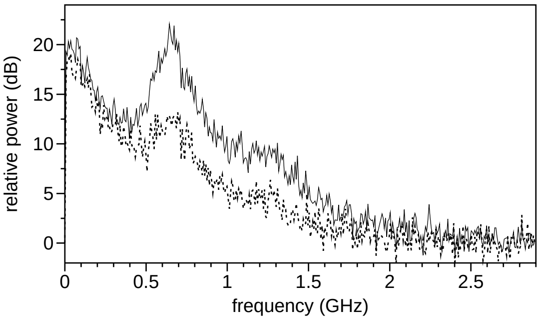

Figure 4. Polarization resolved RF-spectrum at an injection current of 5.21 mA. The spectrum for projection onto the polarization direction corresponding to the mode with lower (higher) optical frequency is denoted by solid (dashed) lines.

If the current is increased, the power of the mode with lower optical frequency surpasses the power of the other mode (5.12 mA), while the power of the mode with higher optical frequency is still increasing. This development continues, until the power of the mode with higher optical frequency reaches a maximum at about 5.2 mA. For further increasing current the power in this mode continuously decreases until it reaches the spontaneous emission level.

From the optical spectrum (Fig. 3) one can extract the dichroism from the difference of the widths (half width at half maximum, HWHM) of the two modes.[5] This method reveals for the device investigated here a dichroism at threshold of about 0.05 GHz (possibly resolution limited) in optical frequency units. Compared to values measured in others of our devices and with data reported in the literature (e.g.[5]), this can be regarded as a rather small value.

In Fig. 4 the polarization resolved RF-spectra are plotted for an injection current close to the current value at which the output power of the mode with higher optical frequency has its maximum value. For both modes, resonances are present in the RF-spectra, which are due to relaxation oscillations ($\nu_{\mathrm{RO}} = 0.65$ GHz). This is a further confirmation that really both modes are lasing. The RF-spectra exhibit also strong noise components at low frequencies and a high frequency tail. The latter is due to the presence of the second harmonic of the relaxation oscillation frequency. The relaxation oscillation peaks occur in both modes as long as the mode with higher optical frequency is above the spontaneous emission level.

In Fig. 6 the HWHM of the relaxation oscillation peak of the mode with lower optical frequency is plotted as a function of current. In linear approximation (i.e. in the small amplitude limit), the HWHM corresponds to the damping rate of the relaxation oscillations. The plot exhibits two different regimes. In each of them the dependence of the damping on current is linear but the slopes are different. The change of slope occurs at a current level of 12% above the lasing threshold. This value coincides with the one at which the mode with higher optical frequency is completely depleted. This indicates that the damping of the relaxation oscillations of the low-frequency mode is somehow affected by the presence of the other mode. However, this observation should be treated with caution, since this behavior has been observed only in one of the devices showing two-mode emission.

Figure 5(a) displays the temporal dynamics at constant current just above the lasing threshold. In both polarization directions bursts starting from the spontaneous emission level are observed. The bursts have amplitudes of an equal order of magnitude for both polarization components and appear with the same probability in a fixed time interval. This resembles the equal time averaged power that is observed at threshold (see Fig. 2). As soon as the power in the mode with lower optical frequency surpasses the power in the other mode, the bursts in the polarization direction corresponding to the mode with higher optical frequency appear less frequently. Simultaneously the amplitude of the bursts of the mode with lower optical frequency increases (Fig. 5b). For this mode also an increase of the DC-level is observed, what is possibly due to the limited bandwidth of the detection system. At further increasing current the bursts in the polarization direction corresponding to the mode with higher optical frequency continuously disappear and the power of that mode remains on the spontaneous emission level.

To analyze the dynamics close to threshold, the cross correlation function of the time traces of the orthogonal polarization modes has been calculated. A typical cross correlation function for the regime of lasing in both modes is plotted in Fig. 7. The cross correlation function reveals a clear anti-correlation of the dynamics in the two polarization directions. The (anti)correlation decays to zero within a few nanoseconds. Furthermore, the cross correlation function is modulated, indicating the existence of a well defined time scale of the fluctuations, and asymmetric with respect to zero time lag.

Figure 8 displays the minimum of the cross correlation functions as a function of the injection current. The amount of anti-correlation exhibits a pronounced dependence on the injection level. Its development with current is qualitative similar to the development of the power of the mode with higher optical frequency, i.e. the maximum anticorrelation is observed at the maximum power of that mode.

To examine the dominating timescale of the polarization dynamics in the regime where both modes are lasing close to threshold, the frequency of the modulation of the cross correlation function in dependence of

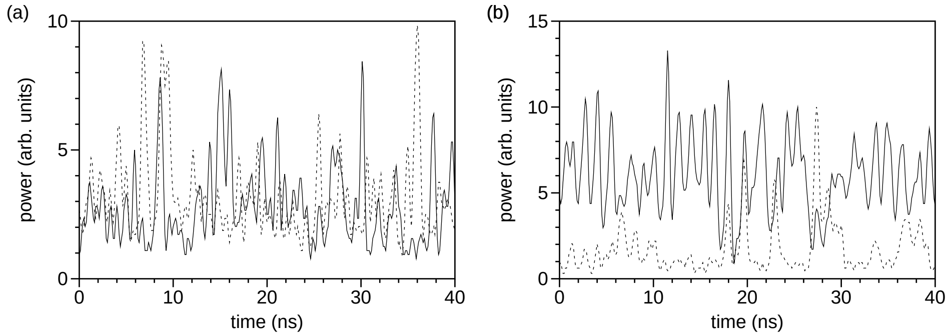

Figure 5. Polarization resolved power at constant current for 5.08 mA (a) and 5.24 mA (b). The power of the mode with lower (higher) optical frequency is denoted by solid (dashed) lines.

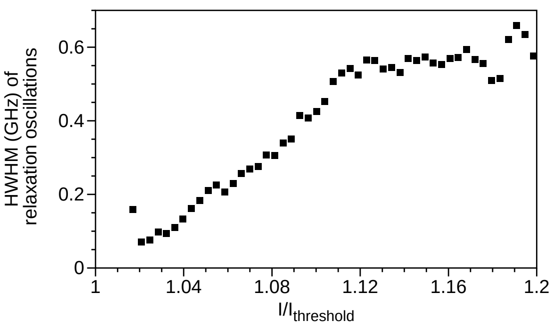

Figure 6. HWHM of the relaxation oscillations of the mode with lower optical frequency in dependence on the injection current.

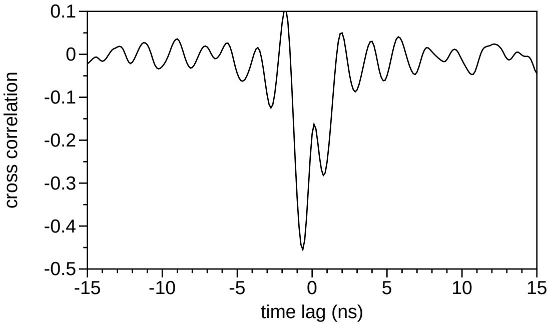

Figure 7. Cross correlation of the two polarization modes for an injection current of 5.2 mA.

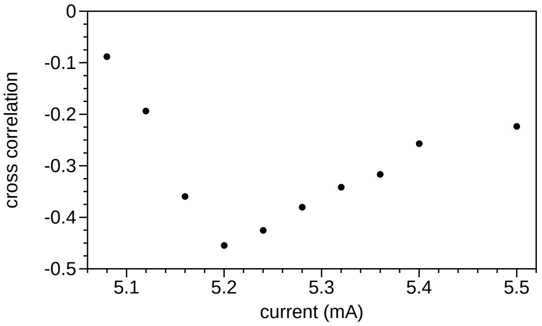

Figure 8. Minimum of the cross correlation function of the time traces of the orthogonally polarized modes in dependence on the injection current.

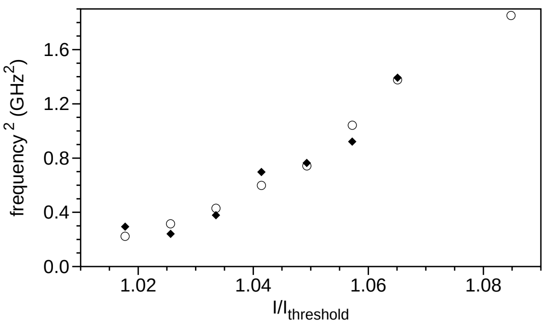

Figure 9. Square of the frequency of the relaxation oscillations (circles) and of the modulation of the cross correlation function (diamonds) of the time series of the polarization modes in dependence on the injection current.

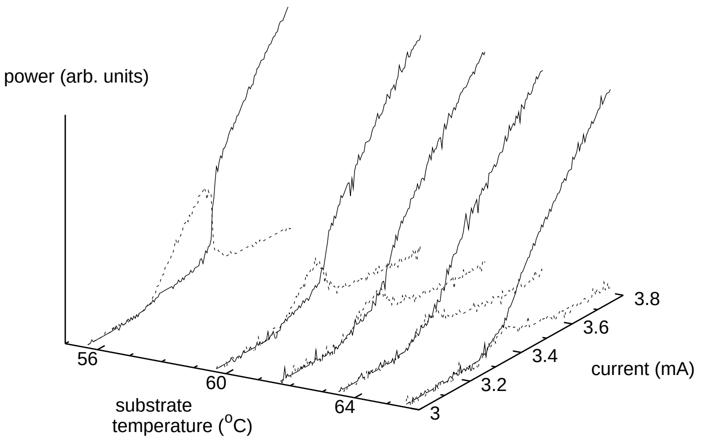

Figure 10. Same as Fig. 2, also in dependence of the substrate temperature and for another device.

the injection current is plotted in Fig. 9 in comparison to the relaxation oscillation frequency. The square of the modulation frequency of the cross correlation function exhibits the same proportionality to the current normalized to threshold as the relaxation oscillations. Furthermore, both frequencies match each other within some fluctuations. From this we conclude that the polarization dynamics at threshold is dominated by the relaxation oscillations.

The dependence of the characteristics of the two-frequency emission state on substrate temperature was studied in another device. Figure 10 shows the polarization resolved output power as a function of injection current and substrate temperature in that laser. At 63°C the same scenario as described above is observed. It remains qualitatively unchanged for increased substrate temperatures up to the maximum recommended operating temperature of 70°C. Also for a slight decrease of substrate temperature no qualitative changes are observed. The dichroism at threshold in this regime of two-frequency emission is low also in this device (≈ 0.1 GHz).

If the substrate temperature is decreased by a critical amount, the laser emits still in both modes at threshold, but with more power in the mode with higher optical frequency (61.5°C). At increasing current, the high-frequency mode is depleted while the power in the orthogonal polarization mode increases continuously. A further decrease of the substrate temperature leads to a further increase of the difference in power of the two modes at threshold. In addition, the current for which the mode with higher optical frequency reaches its maximum power moves to higher values. This development continues, until at threshold only the high frequency mode is lasing (e.g. Fig. 10, 55.5°C). The low frequency mode is not lasing and remains on the spontaneous emission level

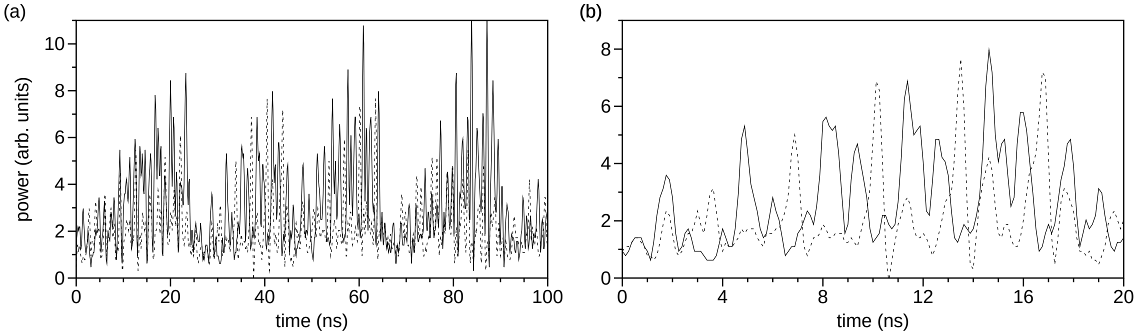

Figure 11. Polarization resolved output power with feedback of -10 dB (threshold reduction 6.4%) at constant current 1% above the solitary laser threshold applied to the device investigated in Fig. 10 at 62°C. The power of the mode with lower (higher) optical frequency is denoted by solid (dashed) lines. Part (b) is a magnification of (a).

until an abrupt polarization switching occurs at higher injection levels. In this operating regime the LI-curve corresponds to the ones reported before in the literature about polarization switching in VCSELs.[3–8, 15]

The transition described above goes along with a continuous change of the dichroism, i.e. the dichroism is increasing with decreasing substrate temperature. The lower the dichroism, the closer to threshold is the polarization switching. If the dichroism is low enough or the point of polarization switching is close enough to threshold, respectively, both modes are lasing at threshold. In conclusion, by a change of the substrate temperature the regime of emission of two lasing modes at threshold is continuously transformed into emission of only the mode with higher optical frequency at threshold and a polarization switching at higher current.

4. DYNAMICS AT THRESHOLD WITH ISOTROPIC OPTICAL FEEDBACK

In this section the dynamics of VCSELs around the solitary laser threshold are studied in the presence of isotropic, mode-matched delayed optical feedback. One – well-known (e.g.[26])– consequence of the feedback is a reduction of the threshold current, with the magnitude of the reduction increasing with the amount of power that is fed back into the laser.

The device investigated first is the same as the one considered in Fig. 10. The operating condition is chosen such that in the solitary laser both polarization modes are lasing at threshold, i.e. the dichroism at threshold is low. Figure 11 displays the dynamics with feedback at constant current slightly above the lasing threshold. In the presence of feedback, in both polarization directions bursts from the spontaneous emission level are observed that are separated by the external cavity round-trip time (3 ns). The amplitude of the bursts is continuously increasing until it abruptly drops to zero. After each dropout, the cycle is repeated. The period of the cycles is rather regular and of the order of several 10 ns. Between the bursts on the external cavity time scale, pulsations with a shorter period are observed that is at the edge of the analog bandwidth of our setup. This behavior resembles the LFF that are well known from edge-emitting lasers (see[24] and references therein).

Under these operating conditions, LFF are observed from current values slightly above the reduced threshold to current values a few percent above the solitary threshold. The period of the LFF-cycles is decreasing with current. Directly at the reduced threshold the dynamics are also dominated by the time scale set by the external cavity, but the temporal evolution of the pulses is not comparable to the typical LFF behavior.

The bursts in the orthogonal polarization directions on the time scale of the external cavity are anticorrelated (see Fig. 12), whereas the dynamics are correlated on the slow timescale of the LFF-cycles, i.e. the LFF-cycles in the orthogonal polarization directions are synchronous. In contrast to the solitary laser the polarization dynamics slightly above the solitary threshold are not governed by the relaxation oscillations.

By changing the substrate temperature to lower values, the dichroism at threshold is increased (see Sec. 3). For an intermediate value of the dichroism (e.g. 0.4 GHz) one of the modes is slightly favored. If in this regime the laser is subjected to isotropic feedback, LFF are observed for the dominant mode. The behavior of the weaker

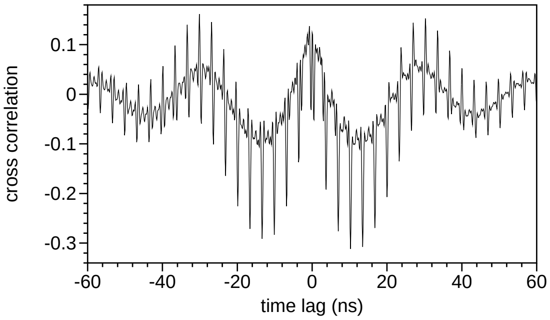

Figure 12. Cross correlation function of the time traces displayed in Fig. 11.

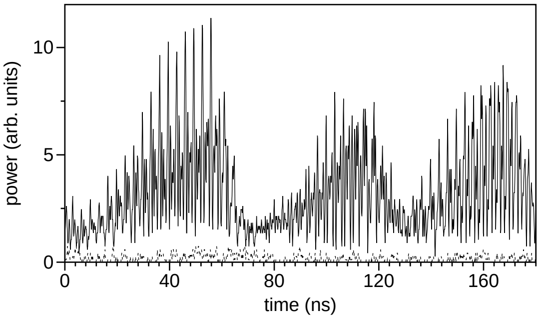

Figure 13. Polarization resolved output power with feedback of -10 dB (threshold reduction 12%) at 96% of the solitary threshold current for a device with large dichroism. The power of the mode with lower (higher) optical frequency is denoted by solid (dashed) lines.

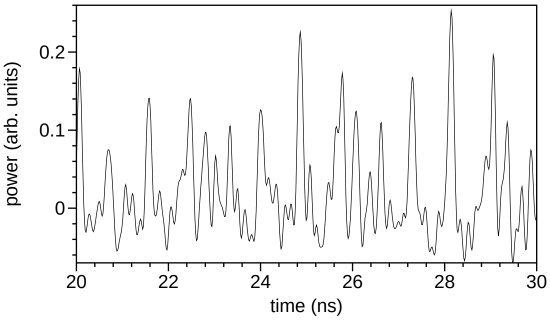

Figure 14. Same as Fig. 13, but with larger bandwidth and without DC components. The graph displays a part of a LFF-cycle at the solitary laser threshold. Only the dominating mode (lower optical frequency) is displayed.

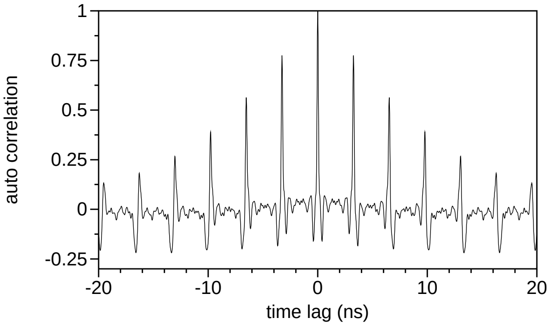

Figure 15. Auto correlation function of the time trace displayed in Fig. 14.

mode is different for different LFF-cycles of the dominant one. The weaker mode can remain on the spontaneous emission level or exhibit LFF with an amplitude lower than for the dominant mode.[27] If LFF occur in both modes, the correlation properties are the same as for low dichroism. In some cycles the weak mode also starts with typical LFF-dynamics, but the amplitude of the pulsations is damped after some point and decreases to zero towards the end of the cycle, whereas the amplitude of the pulsations in the dominant mode is still increasing, i.e. the dynamics of the two modes are anticorrelated on the slow time scale in these cycles.[27] This behavior is similar to the one reported in an earlier publication.[22]

The polarization dynamics with feedback in the vicinity of the solitary threshold for a device with large dichroism (4.5 GHz) are displayed in Fig. 13. Also in this case LFF are observed, but now only for the polarization direction that is also dominating in the solitary laser. The orthogonally polarized mode remains on the spontaneous emission level as is the case without feedback. The current interval of the occurrence of LFF is qualitatively the same as in the low dichroism case. Also the shape of the LFF-cycles and the temporal characteristics in dependence on the injection current are not changed qualitatively.

The temporal dynamics of this laser have also been investigated with a detector of 20 GHz bandwidth and an oscilloscope of 6 GHz analog bandwidth and 20 GSamples/s (Tektronix TDS6604). Due to the small sensitivity of the detector, the signal was amplified by two inverting RF-amplifiers with 20 dB amplification and a bandwidth from 10 MHz to 20 GHz. As a consequence, the DC information of the signals has been lost and a simultaneous measurement of both polarization directions was not possible. A part of a time trace measured with this setup

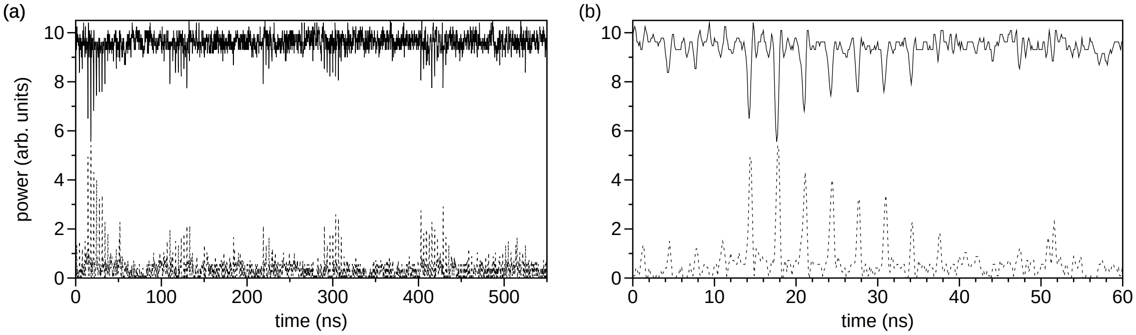

Figure 16. Polarization resolved output power at constant current far above the solitary laser threshold (80%) for the device with large dichroism and a feedback strength of -4 dB. The power of the mode with lower (higher) optical frequency is denoted by solid (dashed) lines. Part (b) is a magnification of (a).

is shown in Fig. 14. The pulsations between two bursts separated by the external cavity round-trip time appear irregularly. This has been confirmed by calculating the auto correlation function of this time trace (Fig. 15). The fast timescale of the irregular pulsations does not occur in the auto correlation function, i.e. the dynamics are clearly dominated by the external cavity time scale.

For the large dichroism case, polarization degrees of freedom are not participating in the dynamics except for feedback strengths greater than -10 dB and current values far above the solitary laser threshold. In this regime, dropouts in the dominating polarization direction occur that are compensated by simultaneous bursts in the weak polarization (Fig. 16). Single dropouts/bursts are separated by the external cavity round-trip time and occur in groups. The polarization dynamics are anticorrelated on the timescale of the external cavity. The grouped fluctuations appear without a defined frequency and are separated by time intervals of approximately 100 ns. These fluctuations are different from the LFF discussed above, since the absolute power does not show a sharp power drop.

5. DISCUSSION AND CONCLUSIONS

In Sec. 3 it has been shown that the dominating time scale in the polarization dynamics in the two-frequency emission state at threshold is given by the frequency of the relaxation oscillations. This is a deterministic time scale. In former publications it has been found that the phenomenon of polarization switching is often accompanied by stochastic, noise driven hopping between the two modes at the switching point.[6, 8] This hopping has been interpreted as the noise-driven transitions between polarization states corresponding to the minima in a double-well potential.[6] The residence times the system stays in one state of polarization have been found to decrease over several orders of magnitude, if the switching point moves closer to the lasing threshold.[6, 8] However, there have been no results published for polarization switchings at current values lower than 20% above threshold. For the two-frequency state at threshold no finite dwell times have been observed. Thus, the transition from polarization switching to the two-frequency state at threshold is also a transition from the dominance of stochastic to the dominance of deterministic time scales and processes.

Fig. 10 shows that – starting from low temperatures – the polarization switching point moves to lower current values, if the temperature is increased. Starting from high temperature, the point at which two-frequency emission gives way to a single, linearly polarized state moves to higher currents, if the temperature is decreased. There seems to be a continuous transformation between the two regions. In this sense, the observed two-frequency emission can be regarded as the manifestation of bistability at threshold. Obviously, for a small enough dichroism none of the two modes is preferred at threshold. Since nonlinear contributions to the dichroism, which are according to the theory developed in[6] responsible for the finite well-depth and the finite dwell-time, will be weak very close to threshold (zero exactly at threshold), other mechanisms might become decisive for polarization dynamics. Our experiments indicate that these are the relaxation oscillations. This has to be clarified in future theoretical work.

In the presence of isotropic feedback again a change of the dominating time scale is observed. The polarization dynamics are now dominated by the external cavity, i.e. the dominating time scale is set by the external cavity round-trip time. This is also the case if no polarization dynamics occur and for strong feedback high above threshold (see Figs. 15 and 16).

From slightly above the reduced lasing threshold up to injection currents a few percent above the solitary laser threshold, LFF are observed in the presence of isotropic feedback. Besides the pulsations at the external cavity round-trip time, also fluctuations on a faster time scale are observed (Fig. 14). However, these fluctuations are uncorrelated. This meets the results of previous investigations on scalar edge-emitting lasers with feedback, which report irregular pulsing on a sub-ns time scale (e.g.[28]). However, we caution that these results are preliminary since the bandwidth of the setup used in our investigations is still limited (6 GHz) and the oscilloscope was only available for a few measurements.

The fact that the occurrence of LFF is observed for different orders of magnitude of the dichroism, suggests, that the LFF appear independent of the polarization dynamics. This is supported by the observation of the LFF in the same current ranges and with the same qualitative characteristics for different dichroism values. For large (low) dichroism, LFF are observed for one (both) of the modes. An intermediate dichroism results in 'mixed' dynamics.[27] Thus, in analogy to the dynamics in the solitary laser, the excitation of polarization degrees of freedom is ruled by the dichroism. As the continuous transition from the two-frequency state to the selection of a 'pure' polarization at threshold in the solitary laser is caused by an increase of the dichroism, the magnitude of the dichroism determines the amount of polarization dynamics in the vicinity of the solitary threshold with isotropic feedback.

In conclusion, in this paper we have given an experimental characterization of the dynamical properties of VCSELs operating close to threshold. For the solitary laser, a state of two lasing modes is observed for low dichroism values. The polarization dynamics of this state are governed by the relaxation oscillations and exhibit a current dependent anticorrelation. A change of the dichroism induced by a change of the substrate temperature results in a continuous transition to the selection of one lasing mode at threshold that is destabilized by a polarization switching at higher currents. With isotropic feedback LFF are observed. The polarization dynamics in the vicinity of the solitary laser threshold in this regime are dominated by the external cavity round-trip time and are anticorrelated on this time scale. The excitation of polarization degrees of freedom in the LFF regime has been shown to depend on the magnitude of the dichroism.

ACKNOWLEDGMENTS

The authors want to thank the Deutsche Forschungsgemeinschaft and the Deutsche Akademische Austauschdienst for financial support. Furthermore, we acknowledge fruitful discussions with S. Balle and J. Mulet on the two-frequency emission state. We are also grateful to Tektronix for the possibility to perform some measurements with the TDS6604.

REFERENCES

1. T. E. Sale, *Vertical Cavity Surface Emitting Lasers*, Research Studies Press Ltd. and John Wiley & Sons Inc., Taunton and New York, 1995.
2. C. J. Chang-Hasnain, J. P. Harbison, G. Hasnain, A. V. Lehmen, L. T. Florez, and N. G. Stoffel, "Dynamic, polarization and transverse mode characteristics of vertical cavity surface-emitting lasers," *IEEE J. Quantum Electron.* **27**, pp. 1402–1409, 1991.
3. K. D. Choquette, D. A. Richie, and R. E. Leibenguth, "Temperature dependence of gain-guided vertical-cavity surface emitting laser polarization," *Appl. Phys. Lett.* **64**, pp. 2062–2064, 1994.
4. J. Martín-Regalado, J. L. A. Chilla, J. J. Rocca, and P. Brusenbach, "Polarization switching in vertical-cavity surface-emitting lasers observed at constant active region temperature," *Appl. Phys. Lett.* **70**, pp. 3350–3352, 1997.
5. M. P. v. Exter, M. B. Willemsen, and J. P. Woerdman, "Polarization fluctuations in vertical-cavity semiconductor lasers," *Phys. Rev. A* **58**, pp. 4191–4205, 1998.

6. M. B. Willemsen, M. U. F. Khalid, M. P. v. Exter, and J. P. Woerdman, "Polarization switching of a vertical-cavity semiconductor laser as a Kramers hopping problem," *Phys. Rev. Lett.* **82**, pp. 4815–4818, 1999.
7. K. Panajotov, B. Nagler, G. Verschaffelt, A. Georgievski, H. Thienpont, J. Danckaert, and I. Veretennicoff, "Impact of in-plane anisotropic strain on the polarization behavior of vertical-cavity surface-emitting lasers," *Appl. Phys. Lett.* **77**(11), pp. 1590–1592, 2000.
8. G. Verschaffelt, J. Albert, M. Peeters, K. Panajotov, J. Danckaert, I. Veretennicoff, H. Thienpont, F. M. d. Sopra, S. Eitel, R. Hoevel, M. Moser, H. P. Zappe, and K. Gulden, "Polarization switching and modulation dynamics in gain- and index-guided vcsels," *Proc. SPIE* **3946**, pp. 246–257, 2000.
9. T. Ackemann and M. Sondermann, "Characteristics of polarization switching from the low to the high frequency mode in vertical-cavity surface-emitting lasers," *Appl. Phys. Lett.* **78**, pp. 3574–3576, 2001.
10. D. V. Kuksenkov, H. Temkin, and S. Swirhun, "Polarization instability and performance of free-space optical links based on vertical-cavity surface-emitting laser," *IEEE Photon. Technol. Lett.* **8**, pp. 703–705, 1996.
11. K. Panajotov, F. Berghmans, M. Peeters, G. Verschaffelt, J. Danckaert, I. Veretennicoff, and H. Thienpont, "Data transparent reconfigurable optical interconnections using polarization switching in VCSEL's induced by optical injection," *IEEE Photon. Technol. Lett.* **11**, pp. 985–987, 1999.
12. A. K. v. Doorn, M. P. v. Exter, and J. P. Woerdman, "Elasto-optic anisotropy and polarization orientation of vertical-cavity surface-emitting semiconductor lasers," *Appl. Phys. Lett.* **69**, pp. 1041–1043, 1996.
13. B. Ryvkin, K. Panajotov, A. Georgievski, J. Danckaert, M. Peeters, G. Verschaffelt, H. Thienpont, and I. Veretennicoff, "Effect of photon-energy-dependent loss and gain mechanisms on polarization switching in vertical-cavity surface-emitting lasers," *J. Opt. Soc. Am. B* **16**, pp. 2106–2113, 1999.
14. K. D. Choquette and R. E. Leibenguth, "Control of vertical-cavity laser polarization with anisotropic transverse cavity geometries," *IEEE Photon. Technol. Lett.* **6**(1), pp. 40–42, 1994.
15. T. Ackemann and M. Sondermann, "Characteristics of polarization switching in vertical-cavity surface-emitting lasers," *Proc. SPIE* **4286**, pp. 44–54, 2001.
16. M. B. Willemsen, A. S. v. d. Nes, M. P. v. Exter, J. P. Woerdman, M. Kicherer, R. King, R. Jger, and K. J. Ebeling, "Polarization-resolved linewidth-power product of a vertical-cavity semiconductor laser," *J. Appl. Phys.* **89**, pp. 4183–4185, 2001.
17. F. Robert, P. Besnard, M. L. Chares, and G. M. Stephan, "Vcsel-polarisation dynamics with polarised feedback," *IEE Proc.-Optoelectron.* **143**(1), pp. 104–106, 1996.
18. F. Robert, P. Besnard, M. L. Chares, and G. M. Stephan, "Polarization modulation dynamics of vertical-cavity surface-emitting lasers with an extended cavity," *IEEE J. Quantum Electron.* **33**, pp. 2231–2238, 1997.
19. B. Li, G. L. Harnagel, and R. R. Craig, "Performance and reliability of high power multi-mode lasers between 0.8 μm and 1 μm," *Proc. SPIE* **3285**, pp. 93–97, 1998.
20. Y. C. Chung and Y. H. Lee, "Spectral characteristics of vertical-cavity surface-emitting lasers with external optical feedback," *IEEE Photon. Technol. Lett.* **3**, pp. 597–599, 1991.
21. S. Jiang, M. Dagenais, and R. A. Morgan, "Spectral characteristics of vertical-cavity surface-emitting lasers with strong external optical feedback," *IEEE Photon. Technol. Lett.* **7**, pp. 739–741, 1995.
22. M. Giudici, S. Balle, T. Ackemann, S. Barland, and J. R. Tredicce, "Effects of optical feedback on vertical-cavity surface-emitting lasers: Experiment and model," *J. Opt. Soc. Am. B* **16**, pp. 2114–2123, 1999.
23. C. H. L. Quay, I. Z. Maxwell, and J. A. Hudgings, "Coherence collapse and redshifting in vertical-cavity surface-emitting lasers exposed to strong optical feedback," *J. Appl. Phys.* **90**(12), pp. 5856–5858, 2001.
24. B. Krauskopf and D. Lenstra, eds., *Fundamental issues of nonlinear laser dynamics*, vol. 548 of *AIP Conference Proceedings*, American Institute of Physics, Melville, 2000.
25. C. Masoller and N. B. Abraham, "Low frequency fluctuations in vertical-cavity surface-emitting semiconductor lasers with optical feedback," *Phys. Rev. A* **59**, pp. 3021–3031, 1999.
26. K. Petermann, "External optical feedback phenomena in semiconductor lasers," *IEEE J. Selec. Top. Quantum Electron.* **1**, pp. 480–489, 1995.
27. M. Sondermann, H. Bohnet, and T. Ackemann, "Low frequency fluctuations and polarization dynamics in vertical-cavity surface-emitting lasers with isotropic feedback," 2002. Preprint, submitted to PRA.

28. I. Fischer, G. H. M. v. Tartwijk, A. M. Levine, W. Elsässer, E. Göbel, and D. Lenstra, "Fast pulsing and chaotic itinerancy with a drift in the coherence collapse of semiconductor lasers," *Phys. Rev. Lett.* **76**, pp. 220–223, 1996.